R. & M. No. 3675

MINISTRY OF AVIATION SUPPLY

AERONAUTICAL RESEARCH COUNCIL
REPORTS AND MEMORANDA

An Approximate Treatment of the Stability of a Towed Unbanked Object in a Condition of Zero Lift

By H. R. Hopkin

Aero Dept., R.A.E. Farnborough

LONDON: HER MAJESTY'S STATIONERY OFFICE
1971
PRICE £1·20 NET

An Approximate Treatment of the Stability of a Towed Unbanked Object in a Condition of Zero Lift

By H. R. Hopkin

Aero Dept.. R.A.E. Farnborough

Reports and Memoranda No. 3675*
April, 1969

Summary.

An approximate method is given for assessing the stability of a towed object, using the same basic theory as Glauert (Ref. 3) and Etkin and Mackworth (Ref. 6). The analysis is developed in terms of lateral stability, but can be simply translated to deal with the longitudinal case. Stability criteria are derived which involve a number of parameters, including the mass and moment of inertia of the body, its drag and transverse aerodynamic force and yawing moment characteristics, and the vertical separation between towed body and the tug. Formulae and charts are given for ready application of the method.

* Replaces R.A.E. Tech. Report No. 69076—A.R.C. 31 359.

LIST OF CONTENTS

---

1. *Introduction.*

Although a number of papers have been written on the general theory of the stability of objects being towed by aircraft, and also on the related inverse problem in which a balloon is tethered by a cable, the application of the theory has been limited. A comprehensive analysis would be complex, even when based on small perturbations and linearised equations, owing to the action of the cable and the aerodynamic forces acting on it, and to the coupling between longitudinal and lateral motions.

The present report is restricted to attempting to generalise and improve the techniques of application of an approximate theory for a drastically simplified mathematical model. To clarify some of the assumptions it seems worthwhile to begin by considering briefly, as background, previous work in the field.

Neumark[1], in examining the aerodynamics of cables for balloons, reviewed the known literature, beginning with Bairstow, Relf and Jones[2]. Much of it relates to the calculation of 'cable derivatives', which are quantities analogous to the familiar derivatives of aerodynamic forces and moments much used in stability analysis. Thus, perturbations in the components of cable force in a purely longitudinal problem would be expressed in the form $X_x x + X_z z$, $Z_x x + Z_z z$, where x, z are components of the displacement of the endpoint of the cable. It is perhaps significant that Glauert[3], Brown[4], Mitchell and Beach[5], and again Neumark came against computational difficulties. The present author, together with H. H. B. M. Thomas, tried recently to extend Neumark's formulae to the doubly limiting case of a cable without weight and without drag. The analysis revealed that, as the limit is approached, the individual derivatives X_x, X_z, Z_x, Z_z tend to infinity but in such a way that $(X_x x + X_z z)$ and $(Z_x x + Z_z z)$ remain finite. This behaviour is the root cause of the computational difficulties. It is, of course, unnecessary to introduce cable derivatives for a weightless dragless cable (which is assumed in the present report), but even in cases in which perturbations in cable forces caused by cable weight and drag do have to be considered, it might be profitable to seek an alternative to a representation in terms of cable derivatives.

The classic paper on the dynamics of towed objects is by Glauert[3]. He considered the shape and dynamics of a light inextensible wire when used for towing, and examined the stability of a towed object subject to assumptions that permitted of separate longitudinal and lateral equations of motion. More recently Etkin and Mackworth[6] produced an analysis, which (although they were unaware of this) corresponded to an approximation given by Glauert. They applied the analysis only to lateral stability. Lipscombe[7] also developed the same sort of theory independently.

Glauert started by determining the shape of the wire following an assumption that the aerodynamic force on an element of length δL would be normal to the element and proportional to $\sin^2 \varepsilon$, where ε is the angle between δL and the airstream. This was based on work by McLeod[8]. Glauert then examined the modes of motion consistent with small perturbations for a wire supporting an object, but assumed at first that the aerodynamic forces acting on the object remained constant during the motion. There were three such modes, which he interpreted as

(a) a transverse 'pendulum oscillation',

(b) a 'pendulum oscillation' in the vertical plane of symmetry,

(c) a 'bowing (or normal) oscillation' in the vertical plane of symmetry.

Finally he added the effect of incremental aerodynamic forces on the towed object, and the equations of motion included terms in X_u, Z_w, Z_q, M_w, M_q and in Y_v, Y_r, N_v, N_r. The separated longitudinal equations yielded a sextic stability polynomial, and, because derivatives of the rolling moment were ignored, the lateral equations yielded a quartic. For typical parameter values, the sextic factorised approximately into a quadratic that always represented a stable mode of motion together with a quartic that was analogous to the lateral quartic, Z_w being considered as the counterpart of Y_v, M_w of $-N_v$, and so on.

Etkin and Mackworth make more drastic assumptions from the outset, as in the present report, which lead directly to the lateral quartic. They have sought corrections to account for the influence of cable drag and mass in approximate fashion, but it seems unwise to toy in such a way with the more general problem, as there is a host of additional interrelated contributions once we depart from the simple straight-cable. Great care must then be taken in making a consistent set of assumptions. They suggest that the simple uncorrected analysis might be accurate enough when the cable drag and mass do not exceed about 10 per cent of those of the towed object, but no positive evidence to support this is known.

The present report makes use only of the simple quartic stability equation, but describes a fairly complete analysis of the consequences of variations in aerodynamic design or moment of inertia of the towed object.

Generalised stability diagrams are outlined, and examples for typical parameter values include a mapping of unstable regions, and give loci that define the maximum degree of instability possible. General expressions for calculating such loci and other quantities are derived. An analysis of the unstable region is important in some applications when the operational pattern cannot completely avoid the region although it may be traversed quite quickly.

Only the equations for lateral motion are given, but as already indicated the basic assumptions are such that the analysis can be applied to the longitudinal motion merely by replacing lateral parameters by corresponding longitudinal ones. For zero aerodynamic forces on the cable the correspondence is exact, and not merely approximate as indicated by Glauert in the general case.

It should be noted that except in some trivial respects the notation follows that described by the author elsewhere[9], and also by the Royal Aeronautical Society[10]. A table of corresponding symbols and expressions used by Glauert[3] and by Etkin and Mackworth[6] is given in the Appendix.

While the present report was being prepared, Pinsker[13] investigated the stability of free-flight model aeroplanes when on tow prior to release. He decided that aerodynamic lift was important and that a good approximation would be obtained by suppressing the yawing freedom but retaining the rolling His stability equation is therefore a quartic that is quite different from the one considered here, and the two reports are complementary.

2. *Equations of Motion.*

Consider an object such that, when towed at a steady speed V_e in level flight, its weight is balanced by the vertical component of the cable tension. The only aerodynamic force is then the drag, which is balanced by the horizontal component of the cable tension. If the cable is inextensible and connected at the centre of gravity, and its mass and drag are negligible, it assumes the shape of a straight line. The configuration in the steady state is depicted in Fig. 1, and perturbations from this state are shown in Fig. 2.

Earth axes $O_o x_o y_o z_o$ provide a reference for the point of cable attachment G and for changes in attitude of the towed object. The origin O_o travels at speed V_e and is always at a distance L from the towing-point P: O_o is also behind and below by amounts a_e, b_e respectively. The vertical separation b_e will be found to have great significance in the motion of the object. The $x_o y_o$ plane is horizontal and the x_o axis is in the vertical plane through O_o.

Any displacement of G relative to O_o is represented by the components x_o, y_o, z_o. Aerodynamic-body axes $Gxyz$ are employed for dealing with the equations of motion, and for defining perturbations in attitude in terms of the deviation angles ϕ, θ, ψ. Since in this application Gxy is horizontal in the datum flight condition, the yaw-deviation angle ψ corresponds to a displacement in a horizontal plane and the pitch-deviation angle θ to one in a vertical plane. The roll-deviation angle ϕ is equal to the bank angle.

Equations of motion are obtained in the usual way, but terms representing the effect of the cable tension have to be included. Consider the components of the tension T in the perturbed state. The components along earth axes are given by the column matrix $\{X_{To}\ Y_{To}\ Z_{To}\}$, or $\{X_{To}\}$ in abbreviated form, where

$$X_{To} = T(a_e - x_o)/L,$$
$$Y_{To} = -T_{y,o}/L,$$
$$Z_{To} = -T(b_e + z_o)/L.$$

The components along body axes are given by

$$\{X_T\} = S\{X_{To}\},$$

where S is the axis transformation matrix.

If we assume perturbations to be small, linearised approximations are forthcoming as follows:

$$S = \begin{bmatrix} 1 & -\psi & \theta \\ \psi & 1 & -\phi \\ -\theta & \phi & 1 \end{bmatrix},$$

$$T = T_e + T', \qquad T' \text{ small},$$

$$X_T = X_{T_e} + X'_T, \quad \text{etc.},$$

$$\{X'_T\} = (I-S)\{T_e a_e/L, \quad O, \quad -T_e b_e/L\} - T_e\{x_o/L, \quad y_o/L, \quad z_o/L\},$$

where I is the unit matrix, or

$$\left.\begin{aligned} X'_T &= T_e(b_e\theta - x_o)/L + a_e T'/L, \\ Y'_T &= -T_e(a_e\psi + b_e\phi + y_o)/L, \\ Z'_T &= T_e(a_e\theta - z_o)/L - b_e T'/L. \end{aligned}\right\} \tag{1}$$

When these force increments are included in linearised equations of motion that could otherwise be separated into two independent sets, longitudinal and lateral, a similar separation is still feasible provided that x_o, z_o, T' are related only to longitudinal variables, and y_o only to lateral ones. The linearising procedure automatically looks after x_o, y_o, z_o, for

$$\dot{x}_o = u, \quad \dot{y}_o = V_e\,\psi + v, \quad \dot{z}_o = -V_e\theta + w,$$

where u, v, w denote the scalar increments in velocity components, and it follows that a separate set of linearised lateral equations is always obtained.

In the more general cause of a curved cable, consistent and reasonable assumptions can be made that also lead to separate lateral and longitudinal linearised equations (*see* Glauert, for example).

The lateral equations of motion used here have a particularly simple form since it is assumed that no rolling motion develops and hence ϕ is zero. The variables are then v, ψ, y_o. Moreover, it is assumed that the cable bears the whole towed weight.

We may proceed at once to normalised forms according to the scheme of Ref. 9. Basic derivatives of aerodynamic forces and moments are aero-normalised, and concise derivatives are dynamic-normalised. The dip overscript ($\breve{}$) and cap ($\hat{}$) are unnecessary, and Y_v will stand for $\breve{Y}_v$, y_v for $\hat{y}_v$, as explained in Ref. 10. The equations of motion in dynamic-normalised form become

$$\begin{aligned} (D + y_v)v + D\psi &= Y'_T, \\ n_v v + (D^2 + n_r D)\,\psi &= 0, \\ Dy_o &= \psi + v, \end{aligned}$$

where all quantities are interpreted in terms of a unit of speed V_e, unit of force $\frac{1}{2}\rho_e V_e^2 S$, unit of time $\tau = \mu l/V_e$, and μ is the relative density parameter $m/\frac{1}{2}\rho_e S l$. Since in the steady state the horizontal and vertical components of the cable tension balance the drag and weight, the second of equations (1) in terms of these units becomes

$$Y'_T = -(C_{De}\,\psi + C_W\phi + y_o/C),$$

where C_{De} is the steady-state drag coefficient,

$$C_W = mg/\tfrac{1}{2}\rho_e V_e^2 S\,,$$

$$C = b_e/\mu l C_W = \frac{b_e V_e^2}{\mu^2 l^2 g}\,. \tag{2}$$

The final form of the equations is therefore, for $\phi = 0$,

$$\left.\begin{aligned} (D+y_v)\,v+(D+C_{De})\,\psi+y_o/C &= 0\,,\\ n_v v+(D^2+n_r D)\,\psi &= 0\,,\\ -v \qquad -\psi+Dy_o &= 0\,. \end{aligned}\right\} \tag{3}$$

The force and moment derivatives are given by

$$y_v = -Y_v = -\frac{\overset{o}{Y}_v}{\tfrac{1}{2}\rho_e S V_e}\,,$$

$$n_v = -\frac{\mu N_v}{i_z}\,, \quad N_v = \frac{\overset{o}{N}_v}{\tfrac{1}{2}\rho_e S l V_e}\,,$$

$$n_r = -\frac{N_r}{i_z}\,, \quad N_r = \frac{\overset{o}{N}_r}{\tfrac{1}{2}\rho_e S l^2 V_e}\,,$$

where i_z is the yawing inertia parameter I_z/ml^2,

and $\overset{o}{Y}_v$, $\overset{o}{N}_v$, $\overset{o}{N}_r$ are derivatives expressed in ordinary dimensional form.

The characteristic or stability equation is the quartic

$$\lambda^4+J_3\lambda^3+J_2\lambda^2+J_1\lambda+J_0 = 0\,, \tag{4}$$

where

$$\left.\begin{aligned} J_3 &= y_v+n_r\,,\\ J_2 &= y_v n_r+\bar{n}_v+1/C\,,\\ J_1 &= C_{De}\bar{n}_v+n_r/C\,,\\ J_0 &= \bar{n}_v/C\,, \end{aligned}\right\} \tag{5}$$

and $\bar{n}_v$ has been written for $-n_v$ as this is usually positive.

3. *Stability Quartic and Stability Boundaries.*

If the aerodynamic forces were negligible, because the speed is low, for example, the quartic would approach the degenerate form $\lambda^2(\lambda^2+J_2)$, where $J_2 = 1/C$ or in ordinary units g/b_e. The factor (λ^2+J_2) would represent a 'pendulum' oscillation with period $2\pi(b_e/g)^{\frac{1}{2}}$. The remaining factor λ^2 merely represents the neutral properties due to the absence of aerodynamic forces.

If, on the other hand, the aerodynamic forces were important but the incremental transverse force Y_T' due to the cable were negligible, the equations of motion would reduce to

$$\begin{aligned} (D+y_v)\,v+D\psi &= 0\,,\\ n_v v+(D^2+n_r D)\,\psi &= 0\,, \end{aligned}$$

which yield the stability equation

$$\lambda^3+(y_v+n_r)\,\lambda^2+(y_v n_r+\bar{n}_v)\,\lambda = 0\,.$$

The factor λ again corresponds to neutral stability, and the remaining quadratic represents a 'directional' mode of motion. Such a mode is usually oscillatory for an aircraft because $\bar{n}_v$ is appreciable on account of a rear fin, and the undamped period is then approximately equal to $2\pi\tau/\omega$, where $\omega^2 = \bar{n}_v$. It will be seen from equations (1) that one way of imagining the condition of zero Y'_T to be approached is to have a very long cable and also to have an object with very small drag/weight ratio, since

$$T_e a_e/L = D_e\,, \qquad T_e b_e/L = W.$$

It is shown later than an undamped oscillation can be present with combinations of b_e and V_e that satisfy the relation $b_e V_e^2$ = constant, and that two such constants exist for any particular towed object. The b_e, V_e plane can therefore be charted into three regions, the one for which motion is unstable being flanked by regions of stability (*see* Fig. 3). The region of instability can be further charted to show the severity of instability.

In order to proceed with the analysis in a generalised form it is useful to change the unit of time by the factor ω, and write $\lambda = \omega s$, so that the stability quartic in terms of s becomes

$$s^4+J_3 s^3+J_2 s^2+J_1 s+J_0\,, \tag{6}$$

where

$$\left.\begin{aligned} J_3 &= (y_v+n_r)/\omega\,,\\ J_2 &= 1+y_v n_r/\omega^2+1/K\,,\\ J_1 &= C_{De}/\omega+n_r/\omega K\,,\\ J_0 &= 1/K\,, \end{aligned}\right\} \tag{7}$$

and

$$K = \omega^2 C\,. \tag{8}$$

Further rationalisation is achieved by introducing the parameters

$$\left.\begin{aligned} f &= n_r/\omega\,,\\ x &= y_v/n_r\,,\\ d &= C_{De}/y_v\,,\\ k &= 1/K = \frac{\mu^2 l^2 g}{b_e V_e^2 \omega^2}\\ &= \frac{\tau}{\omega^2}\frac{g}{b_e}\,, \end{aligned}\right\} \tag{9}$$

since then

$$\left.\begin{aligned} J_3 &= f(1+x)\,,\\ J_2 &= 1+f^2 x+k\,,\\ J_1 &= f(dx+k)\,,\\ J_0 &= k\,. \end{aligned}\right\} \tag{10}$$

It is worth noting that K can also be expressed as $(P_1/P_2)^2$, where P_1 is the basic 'pendulum' period, and P_2 the basic 'directional' period, which were mentioned when discussing the elementary modes for degenerate cases.

In order to determine the critical values of $b_e V_e^2$ we merely have to determine C, or in effect K or k, and the next section discusses the variation of the critical values with f, x, and d.

Stability boundaries.

A mode of motion with zero damping will exist when the stability equation (2–4) has a factor λ or $(\lambda^2 + \text{const.})$. The first possibility corresponds to $\bar{n}_v/C$ being zero, and for finite values of b_e and V_e this implies that $\bar{n}_v$ would have to be zero. The second possibility corresponds to a factor of the form $(s^2 + B_0)$ existing for equation (6), and therefore would require that

$$\left.\begin{aligned} J_0 - J_2 B_0 + B_0^2 &= 0\,, \\ J_1 - J_3 B_0 &= 0\,. \end{aligned}\right\} \tag{11}$$

These are equivalent to the condition

$$B_0^2 - B_0(1 + d - f^2) + d = 0\,, \tag{12}$$

where

$$B_0 = \frac{k + dx}{1 + x}\,. \tag{13}$$

The quadratic in B_0 has rather simpler coefficients than the corresponding quadratic in k, which is

$$k^2 - k\left[(1 + d - f^2) + x(1 - d - f^2)\right] + d(1 + x)(1 + f^2 x) - d^2 x = 0\,, \tag{14}$$

and it is therefore a convenient basis for drawing stability boundaries.

Consider a given towed object with particular values of d, x, f. From (12) we obtain two critical values of B_0, and hence of k by applying (13). By allowing f to vary we can draw in the f, B_0 plane the locus of points corresponding to an undamped oscillation. Two such loci are sketched in Fig. 4, the typical one having a turning point at $B_0 = \sqrt{d}$, $f = 1 - \sqrt{d}$. When $d = 0$ the curve degenerates into two branches: $B_0 = 0$ and $B_0 = 1 - f^2$. The loci reach the B_0-axis at $B_0 = d$ and $B_0 = 1$. An equivalent locus in the f, k plane is shown in Fig. 5. Representative points on the B_0-axis should be interpreted with care, since $fx = y_v/\omega$ and $fdx = C_{De}/\omega$, and the stability quartic for $n_r = 0$ is

$$s^4 + \frac{y_v}{\omega} s^3 + (1 + k) s^2 + \frac{C_{De}}{\omega} s + k = 0\,.$$

When k = d, the factors are

$$(s^2 + d)\left(s^2 + \frac{y_v}{\omega} s + 1\right).$$

As $n_r \to 0$, $x \to \infty$ and the point $f = 0$, $k = 1 + x - dx$ approaches infinity. When k is very large in this way, the stability factors are of the form

$$\left(s^2 + \frac{C_{De} - y_v}{\omega k} s + 1\right)\left(s^2 + \frac{y_v}{\omega} s + k\right),$$

and in the limit become

$$(s^2+1)\left(s^2+\frac{y_v}{\omega}s+\infty\right).$$

Although we may wish to produce a diagram like Fig. 3 for an existing towed object, a generalised form is useful for design purposes, and Fig. 6 seems suitable. Here b_e/g is plotted against $V_e\omega/\mu l$, each corresponding to a particular value of k.

To illustrate the use of Fig. 6, consider a proposed design with $d' = 0{\cdot}04$, $x = 0{\cdot}4$, $f = 0{\cdot}3$. From Fig. 4 we deduce the critical values $B_0 \approx 0{\cdot}04$, $B_0 \approx 0{\cdot}9$, and hence from equation (13) the corresponding $k \approx 0{\cdot}04$, $1{\cdot}25$ (*compare* Fig. 5). In this case, Fig. 6 happens to show curves for $k = 0{\cdot}04$ and $k = 1{\cdot}3$, but if necessary additional curves can be drawn quickly since the equation is merely $[b_e/g]\,[V_e\omega/\mu l]^2 = 1/k$.

4. *Effects of Varying the Aerodynamic Design or Moment of Inertia.*

We have shown that the two stability boundaries given by constant values of $b_eV_e^2$ are determined by the two values of k obtained, for a given value of f, from points such as A, B, in Fig. 5. The aerodynamic parameters considered are the drag coefficient C_{De}, the aero-normalised derivatives Y_v, N_r, N_v, and the moment of inertia I_z. These are contained in the parameters k, f, x, d which appear in the formulae and diagrams of this Report. For convenience, the definitions are collected together below.

$$\begin{aligned}
Y_v &= -y_v, & k &= 1/C\bar{n}_v \quad \text{where } C = b_eV_e^2/\mu^2l^2g, \\
N_r &= -i_zn_r, & f &= n_r/\sqrt{(\bar{n}_v)}, & \bar{n}_v &= -n_v, \\
N_v &= i_z\mu n_v, & x &= y_v/n_r, \\
I_z &= i_zml^2, & d &= C_{De}/y_v.
\end{aligned}$$

We shall first discuss the effects of varying C_{De}, Y_v, N_r, N_v when I_z is constant. Variations of Y_v are reflected in y_v and hence in x and d, those of N_r in n_r and hence in f and x, and those of N_v in $\bar{n}_v$ and hence in k and f.

Variations in C_{De} and Y_v.

Fig. 5 brings out the salient features since the shape of the stability boundary is determined by x and d. It is clear that as d increases towards a value of unity the two critical points on the k-axis approach coincidence, and the whole boundary shrinks towards the point $k = 1, f = 0$. For $d > 1$ the stability boundary reappears with a peak at $f = \sqrt{d}-1$. When $d = 1$ the stability quartic factorises into the form

$$(s^2+fs+1)(s^2+fxs+k),$$

which for positive values of f, x, k represents stable modes of motion. As indicated in Section 3, points on the k-axis have to be considered according to whether f is zero because n_r is zero or $\bar{n}_v$ infinitely large. Thus, if $n_r = 0$ then $f = 0$ but $fx = y_v/\omega$.

In terms of Fig. 3 we conclude that the location of curve B depends directly on x, as it corresponds to the point B in Fig. 5, and that the location of curve A *relative to* curve B depends directly on d. The sensitivity to changes in d is in effect illustrated in Fig. 6, since, as described in Section 3, $k \approx$ d for curve A in many cases.

The main point of design seems to be that the unstable region can be made small by arranging for C_{De} to be comparable with y_v, although considerations of performance and cable characteristics will set a limit in many cases.

Variations in N_v and N_r.

By plotting f^2 against k, as shown qualitatively in Fig. 7, we can represent changes in $\bar{n}_v$, with Cn_r^2 constant, by a point moving along a straight line through the origin 0. This line may intersect the stability boundary at two points such as A, B, and these define the range of $\bar{n}_v$ within which instability would arise. The values of k defining this range are the roots of

$$k^2(1+e+ex)+k\{dx(1+e+ex)-(1+x+d)\}+d(1+x-dx)=0\,, \tag{15}$$

where $e = Cn_r^2$, and the corresponding values of B_0 are the roots of

$$B_0^2(1+e+ex)-B_0(1+d+edx)+d=0\,, \tag{16}$$

where B_0, as before, stands for $\dfrac{k+dx}{1+x}$.

There is a value of e for which the points A, B become coincident, as at T or S. It is obtained more easily from equation (16) than (15), as it must satisfy the condition of equal roots given by

$$(1+d+edx)^2 = 4d(1+e+ex)\,,$$

i.e.
$$(1-d-edx)^2 = 4ed\,,$$

or
$$1-d-edx = \pm 2\sqrt{(ed)}\,.$$

The solution of this equation is

$$\sqrt{(ed)} = \pm\sqrt{\left(\frac{1}{x^2}+\frac{1-d}{x}\right)}\pm\frac{1}{x}\,,$$

which implies two values of e :

$$e = \frac{1}{d}\left[\sqrt{\left(\frac{1}{x^2}+\frac{1-d}{x}\right)}\pm\frac{1}{x}\right]^2 \tag{17}$$

For small values of x and d, e is approximately equal to

$$\frac{1}{d}\left[\frac{2}{x}+\frac{1-d}{2}-\frac{x}{8}\right]^2 \quad \text{or} \quad \frac{1}{d}\left[\frac{1-d}{2}-\frac{x}{8}\right]^2$$

For example, when $x = 0{\cdot}4$, $d = 0{\cdot}04$, these approximations yield $e = 737{\cdot}1$, $4{\cdot}623$, whereas the true values obtained from equation (17) are $740{\cdot}1$, $4{\cdot}864$. These correspond to those given by Glauert on page 20 of Ref. 3, as his equation (63) is equivalent to our (17).

The very large value corresponds to the tangent OS, and the smaller value of OT. We deduce that instability cannot arise when Cn_r^2 lies between $4{\cdot}864$ and $740{\cdot}1$, whatever the value of $\bar{n}_v$. For positive values of $\bar{n}_v$, instability cannot arise when Cn_r^2 exceeds $4{\cdot}864$, or in general

$$\frac{1}{d}\left[\frac{1-d}{2}-\frac{x}{8}\right]^2 \quad \text{approximately.}$$

The inset diagram of Fig. 7 shows the nature of the relevant part of a stability boundary drawn in the

$\bar{n}_v$, C plane. The value of $\bar{n}_v$ below which the motion is always stable corresponds to the point P, that is to the peak on the curve in Fig. 4. This $\bar{n}_v$ is therefore given by

$$\sqrt{(\bar{n}_v)} = \frac{r}{1-\sqrt{d}}.$$

Fig. 8 illustrates results for $x = 0{\cdot}4$, $d = 0{\cdot}04$. The special value of C corresponding to the slope of 4·864 implies a special value of $b_e V_e^2$, which for 'typical' numbers $l = 2$(ft), $\mu = 200$, and $n_r = 4$ comes to about $1{\cdot}5 \times 10^6$. Thus for a modest cable length, say $b_e = 100$ (ft), the speed must exceed about 122 ft/s. On the other hand, we can say that the motion is stable for all values of b_e and V_e provided that $n_r/\sqrt{(\bar{n}_v)}$ is greater than 0·8. Although this sort of value may be impossibly large for a given towed object, there could be considerable design freedom when the object is a carrier of goods or equipment, and then arrangements of forward and rear fins which are unusual in aeroplanes might achieve a favourable value of $n_r/\sqrt{(\bar{n}_v)}$. The fins might well be dorsal and ventral and extend along a considerable length of the body.

The use of larger fins to increase n_r will also result in an increase of y_v, so that the value of x is unlikely to change very much. In terms of Fig. 5, we see that the critical value $k = 1+x-dx$ is therefore also unlikely to change significantly.

The total damping available to be shared among the modes of motion (typically two oscillations somewhat analogous to the pendulum and directional modes described in Section 3) is $(y_v - n_r)$, so that a large value in relation to $\sqrt{(\bar{n}_v)}$ would be expected to be beneficial. A very low value of $\bar{n}_v$ would cause the towed object to tend to wander about, as a poorly damped exponential mode of motion would be present.

Variation in I_z.

For a given aerodynamic design n_r and n_v are inversely proportional to the moment of inertia I_z, and hence $f^2 \propto 1/I_z$ whereas $k \propto I_z$. It follows that an increase in I_z can be represented by a point moving from left to right along a rectangular hyperbola $f^2 k =$ constant superimposed on Fig. 7. An increase in the moment of inertia therefore improves stability if the original value corresponds to a point in the vicinity of the right hand branch of the stability boundary, but diminishes stability if the original point is near the left hand branch.

5. *Mapping of Unstable Region.*

An analysis of the unstable region may be beneficial. As we have seen from Fig. 3, the unstable region, when it exists, stretches to infinity in the directions of both axes. In applications where either cable length or speed have a range of values it may then be impossible to avoid spending some time in a potentially unstable condition. Strictly speaking, we cannot apply a stability diagram that relates to constant datum values to a condition in which parameters vary continuously, but it is reasonably safe to assume that the likelihood of building up an oscillation, while traversing a region that has been labelled unstable from a panlinear† analysis, is a function of the degree of instability predicted by that same analysis.

For the stability equation considered in this Report it is found that the degree of instability increases as we penetrate further into the region between curves A and B in Fig. 3, but there is a definite limit and a locus of maximum instability exists within the region, as illustrated in Fig. 9 by the heavy dashed curve.

In preparing such a diagram it is assumed that the stability equation (6) has a factor $(s^2 - As + B)$, which corresponds to a growing oscillatory mode with persistence index $\sigma = \frac{1}{2}A$, and angular frequency $(B-\sigma^2)^{\frac{1}{2}}$, expressed in the special time scale associated with s. In other words the mode has the form $\exp(\sigma t^*) \sin[(B-\sigma^2)^{\frac{1}{2}} t^* + \varepsilon]$, where $t^* = \omega t/\tau$.

---

†It has been proposed by Hopkin and Thomas[11] that linear differential equations with constant coefficients be called panlinear.

In Fig. 9 the curves numbered 1, 2, 3, 4 are respectively loci of constant persistence given by $A = 0$, 0·025, 0·05, and 0·0654 (max), and one striking feature is the disparity in the gradients as we proceed inwards from the two stability boundaries. This was taken to be the explanation of an apparent disagreement between theory and experiment in a particular case. Excellent agreement was obtained in mapping out the lower stability boundary but not the upper one. Th[8] discrepancy, however, seemed hardly surprising when theory predicted a very low rate of change of A in the vicinity of the upper boundary, as the difficulties inherent in pinpointing a condition of zero damping by experiment would be increased considerably.

It is interesting to draw contours of constant persistence within the framework of Fig. 5 or Fig. 4, and an example is illustrated by Fig. 10. We find that the loci of constant A are closed curves that converge to a point P representing the peak value of A. This is of course not the maximum value referred to in Fig. 9, because in that example the value of f was fixed at 0·3. The loci in Fig. 9 thus correspond to the points 1, 2, 3, 4 in Fig. 10. For an existing design the value of f would be known, and a diagram like Fig. 9 might be drawn. During a design study, however, it might be worth determining the point P, as this corresponds to the worst possible combination of parameters as far as stability is concerned. The equations that are required for carrying out this work are given in Appendix 2 and illustrated by Figs. 10 to 13.

6. *Modes of Motion.*

It is illuminating to try and identify the nature of the two typical modes of iscillation. Working in our special time scale, we correlate a separate pendulum mode with a factor (s^2+k) and a separate directional mode with $[s^2+f(1+x)s+(1+f^2x)]$.

Consider the stability factors and values of k associated with the points 1, 2, 3, 4, 3, 2, 1 on Fig. 10, as follows.

Factors	k
$(s^2+0{\cdot}0442)(s^2+0{\cdot}42s+1{\cdot}038)$	0·0459
$(s^2-0{\cdot}025s+0{\cdot}2486)(s^2+0{\cdot}445s+1{\cdot}063)$	0·2642
$(s^2-0{\cdot}05s+0{\cdot}4336)(s^2+0{\cdot}47s+1{\cdot}119)$	0·4851
$(s^2-0{\cdot}0654s+0{\cdot}6346)(s^2+0{\cdot}4854s+1{\cdot}185)$	0·7522
$(s^2-0{\cdot}05s+0{\cdot}7837)(s^2+0{\cdot}47s+1{\cdot}289)$	1·0102
$(s^2-0{\cdot}025s+0{\cdot}8594)(s^2+0{\cdot}445s+1{\cdot}335)$	1·1476
$(s^2+0{\cdot}9058)(s^2+0{\cdot}42s+1{\cdot}382)$	1·252

For the values taken ($f = 0{\cdot}3$, $x = 0{\cdot}4$, $d = 0{\cdot}04$) the basic directional mode corresponds to $(s^2+0{\cdot}42s+1{\cdot}036)$, and for the left hand point 1 we can thus be safe in calling the undamped mode a pendulum mode. The position is not clear, however, as k becomes larger and of the order of unity, since the basic modes then have very similar frequencies. It is tempting to say that the two points on the stability boundary correspond to a pendulum-type mode (small k) and a directional-type mode ($k \approx 1$), these being associated in turn with the lower and upper boundaries in Fig. 3 and Fig. 9. It is unwise, however, to guess in this way, and a more reliable basis would be to observe or calculate the dynamic behaviour. Perhaps we could go so far as to say that it would not be surprising if a more complicated motion—a combination of pendulum swinging and yawing oscillation—were obtained for a large critical value of k in contrast to a more nearly pure pendulum motion for a small critical value of k.

7. *Discussion and Conclusions.*

Although the analysis developed in the present report is based on drastic simplifying assumptions, there is evidence that it forms a valuable guide for avoiding or remedying designs that result in unstable

oscillation of a towed object at certain combinations of cable length and towing speed. Many aspects of the theory were found to be realistic in recent work by Mettam[12] and in associated work in France, to which he refers.

The existence of stable or unstable motion depends on the relative values of the normalised parameters y_v, n_v, n_r, C_{De} and a quantity $C = b_e V_e^2/\mu^2 l^2 g$, so that it is impossible to discuss briefly all the significant combinations. A general stability boundary can, however, be drawn (Fig. 4). This shows the great importance of the quantities $f = n_r/\sqrt{(\bar{n}_v)}$, $d = C_{De}/y_v$. The one factor that can reduce the unstable region to zero is the ratio C_{De}/y_v, the value unity being the best.

The benefits from other variations in aerodynamic design or moment of inertia are less definite and have to be studied in detail, as modifications to the body or tail (or fin) can significantly affect all the parameters at the same time. It is possible in principle to ensure complete stability (subject of course to the basic assumptions), for all combinations of cable length and towing speed, by designing $n_r/\sqrt{(\bar{n}_v)}$ to be greater than $1-(C_{De}/y_v)^{\frac{1}{2}}$, but this much freedom of design may not be available in a particular application†.

If an unstable region exists as illustrated in Fig. 3, it may nevertheless be possible to operate wholly within the lower stable area or the upper stable area. On the other hand it may be necessary to operate in the one or the other at different times during the same flight. If this be so, a flight procedure might be found such that the growth of an oscillation is acceptably slow while the transition through the unstable region is carried out. For example, it could be beneficial to lengthen the cable while the speed is low enough to maintain stable conditions, and then increase speed so as to reach the upper stable region after crossing a relatively narrow unstable band. Another possibility is to raise or lower the towed object while the speed is high, as this also corresponds to a narrow band of instability. In a given case the maximum degree of instability and the period of oscillation should be calculated in terms of ordinary time units in order to asses the nature of the modes of motion likely to be encountered while the unstable region is traversed.

†If $C_{De} > y_v$ the critical value of $n_r/\sqrt{(\bar{n}_v)}$ is $(C_{De}/y_v)^{\frac{1}{2}} - 1$.

LIST OF SYMBOLS

A	=	2σ (coefficient of $-s$ in quadratic stability factor)
A_m		Maximum value of A for specified f
A_M		Peak maximum value of A
a_m	=	A_m/J_3 (normalised value of A_m)
a_e		Horizontal separation between towed object and towing aircraft in steady flight
a_1		$1+a_m$
B		Constant coefficient in quadratic stability factor
B_m		Value of B when $A = A_m$
B_o		Value of B when $A = 0$
b_e		Vertical separation between towed object and towing aircraft in steady flight
b_1		$1-B_m$
C	=	$b_e V_e^2/\mu^2 l^2 g$
C_{De}		Drag coefficient of towed object in steady flight
C_W		Normalised weight, $W/\frac{1}{2}\rho_e V_e^2 S$
D		Differential operator with respect to time
d	=	C_{De}/y_v
d_1	=	$1-d$
e	=	Cn_r^2
F	=	$1/f$
F_i		Coefficients of quadratic in F_m $(i = 0, 1, 2)$
f	=	n_r/ω
G_i		Coefficients of cubic in f $(i = 0, 1, 2)$
g		Acceleration due to gravity
H_i		Coefficients of sextic in A_m $(i = 0, 1, 2, 3, 4, 5, 6)$
J_i		Coefficient of stability quartic $(i = 0, 1, 2, 3)$
K	=	$C\bar{n}_v = C\omega^2 = P_1^2/P_2^2$
k	=	$1/K$
I_z		Moment of inertia of towed object about z-axis
i_z		Yawing inertia parameter (normalised value of I_z), $i_z = I_z/ml^2$
L		Length of towing cable (constant)
l		Representative length
m		Mass of towed object
N_v, N_r		Aero-normalised derivatives of yawing moment

n_v, n_r — Concise dynamic-normalised counterparts of N_v, N_r ($n_v = -\mu N_v/i_z$, $n_r = -N_r/i_z$)

$\bar{n}_v = -n_v = \omega^2$

r — Yawing component of angular velocity

S — Representative area

S — Axis transformation matrix

s — Root of stability equation, $s = \lambda/\omega$

$P_1 = 2\pi(b_e/g)^{\frac{1}{2}}$, period of free pendulum mode

$P_2 = 2\pi\mu l/\omega V_e$, approximate period of free directional mode

T — Tension in towing cable

t — Time in ordinary units

t^* — Time in special units, $\omega t/\tau$

$u(F)$ — Function used for determining a_m (*see* Section 5)

V — Resultant speed of towed object (associated with vector V)

V_e — Value of V in steady datum flight condition

v — Component of $\vec{V}$ along y-axis

W — Weight of towed object

$X = 1/x$

X_T, Y_T, Z_T — Components of cable tension T along body axes

X_{To}, Y_{To}, Z_{To} — Components of cable tension T along normal earth axes

X_i — Coefficients of quadratic in x_m ($i = 0, 1, 2$)

$x = y_v/n_r$

x_o, y_o, z_o — Components (along normal earth axes) of displacement of body-axes origin relative to position in steady flight

Y_v — Aero-normalised derivative of transverse force

y_v — Concise dynamic-normalised counterpart of Y_v ($y_v = -Y_v$)

Z_i — Coefficients of quadratic in z ($i = 0, 1, 2$)

$z = A_m/(1-d)$

θ — Pitch-deviation angle

λ — Root of stability polynomial for dynamic-normalised equations, $\lambda = \omega s$

μ — Relative density parameter, $m/\frac{1}{2}\rho_e Sl$

ρ_e — Ambient air density for steady datum flight condition

σ — Persistence index of oscillatory mode of motion

τ — Dynamic-normalised unit of time, $m/\frac{1}{2}\rho_e SV_e$

ϕ		Roll-deviation angle
ψ		Yaw-deviation angle
ω	=	$\sqrt{(\bar{n}_v)}$ (approximate angular frequency of free directional mode in dynamic-normalised units)

Suffixes

e	Datum values
m	Values corresponding to maximum persistence index
M	Values corresponding to peak maximum persistence index
o	Components along normal earth axes $0_o\ x_o\ y_o\ z_o$

Superfix

T' denotes increment in $T (T = T_e + T')$, and so on

Overscript

$\cdot$	$\dot{x}$ denotes dx/dt, and so on
$-$	$\bar{n}_v$ denotes $-n_v$
o	Identifies derivatives in ordinary units

REFERENCES

No.	*Author(s)*	*Title, etc.*
1	S. Neumark	Equilibrium configurations of flying cables of captive balloons, and cable derivatives for stability calculations. A.R.C. R. & M. 3333 (1961).
2	L. Bairstow, E. F. Relf and R. Jones . .	The stability of kite balloons: mathematical investigation. A.R.C. R. & M. 208 (1915).
3	H. Glauert	The stability of a body towed by a light wire. A.R.C. R. & M. 1312 (1930).
4	L. W. Bryant, W. S. Brown, and N. E. Sweeting . .	Collected researches on the stability of kites and towed gliders. A.R.C. R. & M. 2303 (1942).
5	K. Mitchell and C. Beach . .	The stability derivatives of a glider towing cable, with a method for determining the flying conditions of the glider. R.A.E. Report Aero 1764 (A.R.C. 6151) (1942).
6	B. Etkin and Jean C. Mackworth	Aerodynamic instability of non-lifting bodies towed beneath aircraft. Univ. of Toronto Inst. of Aerophysics. Technical Note 65 (1963).
7	J. Lipscombe	Preliminary investigations into the instability of a small helicopter-towed body. Min. Defence (Navy Dept) unpublished report (1966).

8 A. R. McLeod . . . . . On the action of wind on flexible cables, with applications to cables towed below aeroplanes and balloon cables.
A.R.C. R. & M. 554 (1918).

9 H. R. Hopkin . . . . . A scheme of notation and nomenclature for aircraft dynamics and associated aerodynamics.
A.R.C. R. & M. 3562 (1966).

10 Dynamics Committee . . . . Engineering Sciences Data, Aeronautical Series, Dynamics Sub-Series.
(Royal Aeronautical Society)
Issue 1 (Items 67001 to 67007) (February, 1967).

11 H. R. Hopkin and . . . . Proposed terms for describing some properties of physical systems·
H. H. B. M. Thomas
R.A.E. Tech. Memo Aero 997 (A.R.C. 29658) (1967).

12 A. R. Mettam . . . . . Wind tunnel investigations of instability in a cable-towed body system.
R.A.E. Tech. Report 69022 (1969).

13 W. J. G. Pinsker . . . . The stability of towed free-flight models.
A.R.C. R.& M. 3641 (1968).

APPENDIX 1

Corresponding Quantities in Three Notations.

This Report	Etkin & Mackworth[6]	Glauert[3]
Y_v	$C_{y_\beta} = Y_v$	
N_v	$C_{n_\beta} = N_v$	
N_r	$C_{n_r} = 2N_r$	
l	b	$l = [\sqrt{mR}/\rho V]$
S	S	$l^2 (= GS$ say)
ρ_e	ρ	ρ
$\mu = m/\frac{1}{2}\rho_e Sl$	$\mu = m/\frac{1}{2}\rho Sb$	$\mu = m/\rho l^3$
i_z	$k_z^2/b^2 = i_z$	
V_e	u_o	V
$\tau = m/\frac{1}{2}\rho_e V_e S$	$t^* = b/2u_o$	$[m/R]^{\frac{1}{2}} = \tau/2G$
λ/τ	$\hat{\lambda}/t^*$	$\lambda/[m/R]^{\frac{1}{2}}$
C_{De}	C_{Do}	$k_D = \frac{1}{2} C_{De}/G$
$y_v = -Y_v$		$y_v = -\frac{1}{2} Y_v/G$
$\bar{n}_v = \mu N_v/i_z$		$\mu n_v = -\frac{1}{4} \bar{n}_v/G^2$
$n_r = -N_r/i_z$		$n_r = \frac{1}{2} N_r/i_z G$
b_e	h	b
a_e	a	
$x = y_v/n_r$	$2k_z^2 C_{y_\beta}/b^2 C_{n_r}$	y_v/n_r
$d = C_{De}/y_v$	$-C_{Do}/C_{y_\beta}$	k_D/y_v
$f = n_r^2/\bar{n}_v$	$b^2 C_{n_r}^2/4k_z^2 \mu C_{n_\beta}$	$-n_r^2/\mu n_v$
$C = b_e V_e^2/\mu^2 l^2 g$	$Fh/b\mu^2$	$\dfrac{\sec\phi}{\gamma} = 4GC$

APPENDIX 2

Contours of Constant Persistence and Loci of the Maximum Persistence.

The following conditions must be satisfied in order that $(s^2 - As + B)$ should be a stability factor.

$$\left.\begin{aligned} J_0-(J_2+J_3A+A^2)\,B+B^2 &= 0\,,\\ (J_1+J_2A+J_3A^2+A^3)-(J_3+2A)\,B &= 0\,. \end{aligned}\right\} \tag{A.2.1}$$

The second of these equations is linear in k and B:

$$B\Big[(f+A)+(fx+A)\Big] = k(f+A)+(fdx+A)+A(f+A)\,(fx+A)\,. \tag{A.2.2}$$

We can therefore derive a quadratic in either k or B, with coefficients that are functions of f, x, d, A. In the case $A = 0$ we have shown that the quadratic in B is simpler than the k quadratic, and this is also what happens when A is not zero.

We find that

$$(fx+A)\,B^2-\Big[(fx+A)+(fdx+A)-f(fx+A)\,(f+A)\Big]B+\Big[(fdx+A)+A(fx+A)\,(f+A)\Big] = 0\,, \tag{A.2.3}$$

and this equation reduces, as it should, to (12) when $A = 0$.

The two values of B correspond to pairs of points such as 1, 1 and 2, 2 in Fig. 10, and A_m, the maximum value of A, therefore corresponds to two equal values of B. The condition for equal values reduces to

$$f^2x^2(1-d)^2+2Tf^2x(1-d)+(f^2-4)\,T^2 = 0\,,$$

where $T = (f+A_m)\,(fx+A_m)$, and hence to

$$\Big[fx(1-d)+(f-2)\,T\Big]\Big[fx(1-d)+(f+2)\,T\Big] = 0\,.$$

There are two possibilities:

$$fx(1-d)+(f\pm 2)\,T = 0\,, \tag{A.2.4}$$

with associated values for B and k:

$$\left.\begin{aligned} B_m &= 1\pm(f+A_m)\,,\\ k_m &= \Big[1\pm(f+A_m)\Big]\Big[1\pm(fx+A_m)\Big] \end{aligned}\right\} \tag{A.2.5}$$

For positive f, x, A_m we must have $T > 0$, and hence the possibilities reduce to the following.

$$\text{For } d<1: \qquad \left.\begin{aligned} &fx(1-d)+(f-2)\,T = 0\,,\\ &B_m = 1-f-A_m\,,\\ &k_m = B_m(1+fx+A_m)\,. \end{aligned}\right\} \tag{A.2.6}$$

$$\text{For } d>1: \qquad \left.\begin{aligned} &fx(1-d)+(f+2)\,T = 0\,,\\ &B_m = 1+f+A_m\,,\\ &k_m = B_m(1-fx-A_m)\,. \end{aligned}\right\} \tag{A.2.7}$$

To examine the case $d = 1$ we must return to equation (20), which then becomes

$$(B-1)\left[B-1-f(f+A)\right] = 0,$$

so that it is impossible to have equal roots except when $f = 0$.

Only the case $d < 1$ is considered here in more detail, as this applies to a large variety of towed objects and furthermore the analysis for $d > 1$ may be produced quickly by analogy. For objects designed to have little drag a typical value of d is less than 0·1, and quite draggy shapes have values less than unity.

The first of equations (A.2.6) can be expressed in a slightly different form to enable the drawing of generalised curves. Written in full the equation is

$$A_m^2 + A_m f(1+x) + f^2 x + \frac{fx(1-d)}{f-2} = 0, \tag{A.2.8}$$

and if we write $A_m = a_m J_3 = a_m f(1+x)$, we obtain the equivalent equation

$$\left[a_m^2 + a_m\right]\left[x + \frac{1}{x} + 2\right] = \frac{(F-1)^2 - F^2 d}{2F-1} = u(F) \tag{A.2.9}$$

where F stands for $1/f$. For given values of a_m and d, we can therefore draw a curve relating F and x. A curve of more general applicability is, however, obtained by plotting the function $u(F)$ and F. This is done in Fig. 11, for $d = 0$ and $d = 0{\cdot}04$, and it is seen that there are two asymptotes: one given by $F = \frac{1}{2}$ and another by

$$u(F) = \tfrac{1}{2}F(1-d) - \tfrac{1}{4}(3+d).$$

The alternative of drawing families of curves relating F and x is illustrated by Figs. 12 and 13. The abscissa is $(x + 1/x)$ but an equivalent scale for x is also given. Since the minimum value of $(x + 1/x)$ is 2, and f is known to be less than $(1 - \sqrt{d})$ in the unstable region, we need look only at one branch of the curve. This corresponds to the upper branch in Fig. 11.

Curves have been drawn for $a_m = 0$, 0·1, 0·2, 0·4 for both $d = 0$ and $d = 0{\cdot}04$. A value of 0·4 for a_m represents a large degree of instability, in that one oscillatory mode has procured 140 per cent of the total system damping (J_3) leaving the other mode unstable with -40 per cent. For the range of values considered the asymptotes provide good approximations, but the exact expressions are not unwieldy.

One interesting conclusion is that $(x + 1/x)$ appears as a significant quantity, and that x, the ratio of y_v and n_r, can vary over the typical range 0·5 to 1·0 without altering $(x + 1/x)$ very much. Variation of f is much more important.

In order to work backwards and predict what values of x and f would produce a specified a_m and B_m for a given d, we may use the relation

$$b_1 F_m = a x_m + a_1, \tag{A.2.10}$$

where

$$\left.\begin{aligned} a_1 &= 1 + a_m \\ b_1 &= 1 - B_m, \end{aligned}\right\} \tag{A.2.11}$$

together with a quadratic equation for either x_m or F_m, namely

$$X_2 x_m^2 + X_1 x_m + X_o = 0, \tag{A.2.12}$$

$$F_2F_m^2+F_1F_m+F_o = 0\,, \tag{A.2.13}$$

where

$$X_2 = 2a_1b_1-1+d\,, \qquad F_2 = X_2\,,$$
$$X_1 = 2ab_1+a_1(X_2-b_1^2)/a\,, \qquad F_1 = 2a^2-a_1b_1-a_1F_2/b_1\,,$$
$$X_0 = b_1(2a_1-b_1)\,, \qquad F_0 = 1+2a\,.$$

Determination of the peak value of A.

The typical diagram Fig. 10 shows two values of f corresponding to a maximum and a minimum on each locus of positive constant A, so long as A is less than the value at the peak P. At the peak the maximum and minimum have coalesced, and the condition for this is that equation (A.2.8) must be satisfied by two equal values of f. Writing the equation as a cubic

$$f^3-G_2f^2-G_1f-G_0 = 0\,, \tag{A.2.14}$$

we express the condition for two equal roots as

$$-4G_1^3+4G_2^3G_0+27G_0^2+18G_2G_1G_0-G_2^2G_0^2 = 0\,. \tag{A.2.15}$$

The G coefficients are given by

$$G_2 = 2-yA_m\,,$$
$$G_1 = 2yA_m-d_1-XA_m^2\,,$$
$$G_0 = 2XA_m^2\,,$$

where $X = 1/x$, $y = 1+X$, $d_1 = 1-d$.
The result of substituting in the condition (A.2.15) is a sextic

$$H_6A_m^6+H_5A_m^5+ \ldots\ldots\ldots +H_1A_m+H_0 = 0\,, \tag{A.2.16}$$

and the peak value A_M is a root of this equation. The H coefficients are given by

$$H_6 = X^2(4X-y^2)\,,$$
$$H_5 = 4Xy(4X-y^2)\,,$$
$$H_4 = X^2(32+12d_1)+y^2(8X-4y^2-2d_1X)\,,$$
$$H_3 = 16y(4X-y^2)+4d_1y(y^2-X)\,,$$
$$H_2 = 16(4X-y^2)-d_1X(80-12d_1)+d_1y^2(32-d_1)\,,$$
$$H_1 = d_1y(16-20d_1)\,,$$
$$H_0 = -4d_1^2d\,.$$

For problems where A_M is small some of the terms in equation (A.2.16) could be ignored in order to furnish an approximation. One such approximation is a root of the quadratic

$$Z_2z^2+Z_1z+Z_0 = 0\,, \tag{A.2.17}$$

where

$$A_m = (1-d)z\,, \tag{A.2.18}$$

and

$$Z_2 = 15y^2 - 4X + d(56X - 30y^2)\,,$$
$$Z_1 = -4y(1-5d)\,,$$
$$Z_0 = -4d\,.$$

As an example consider $x = 0{\cdot}4$, $d = 0{\cdot}04$. The coefficients of the sextic become

$H_6 = -14{\cdot}0625$, $H_5 = -78{\cdot}75$, $H_4 = -142{\cdot}05$, $H_3 = -5{\cdot}04$
$H_2 = 164{\cdot}6784$, $H_1 = -10{\cdot}752$, $H_0 = -0{\cdot}147456$,

and there is a root $+0{\cdot}07713$ as indicated in Fig. 10. The approximate quadratic is

$$164{\cdot}6784\,z^2 - 11{\cdot}2\,z - 0{\cdot}16 = 0\,,$$

i.e.

$$164{\cdot}6784\,(z + 0{\cdot}012124)\,(z - 0{\cdot}080135) = 0\,.$$

The root $0{\cdot}080135$ corresponds to $A_m = 0{\cdot}080135 \times 0{\cdot}96 = 0{\cdot}07693$, and this differs from the true A_M by just $0{\cdot}0002$.

It is interesting to note that as d approaches zero, the approximate quadratic approaches

$$(15y^2 - 4X)\,z^2 - 4yz = 0\,,$$

and the root we are seeking approaches the value $4y/(15y^2 - 4X)$. At the same time $z \to A_M$. For the example considered above the limiting value is $14/173{\cdot}75$, i.e. $0{\cdot}0806$, so it seems likely that the limit would provide quite a good approximation when d is small.

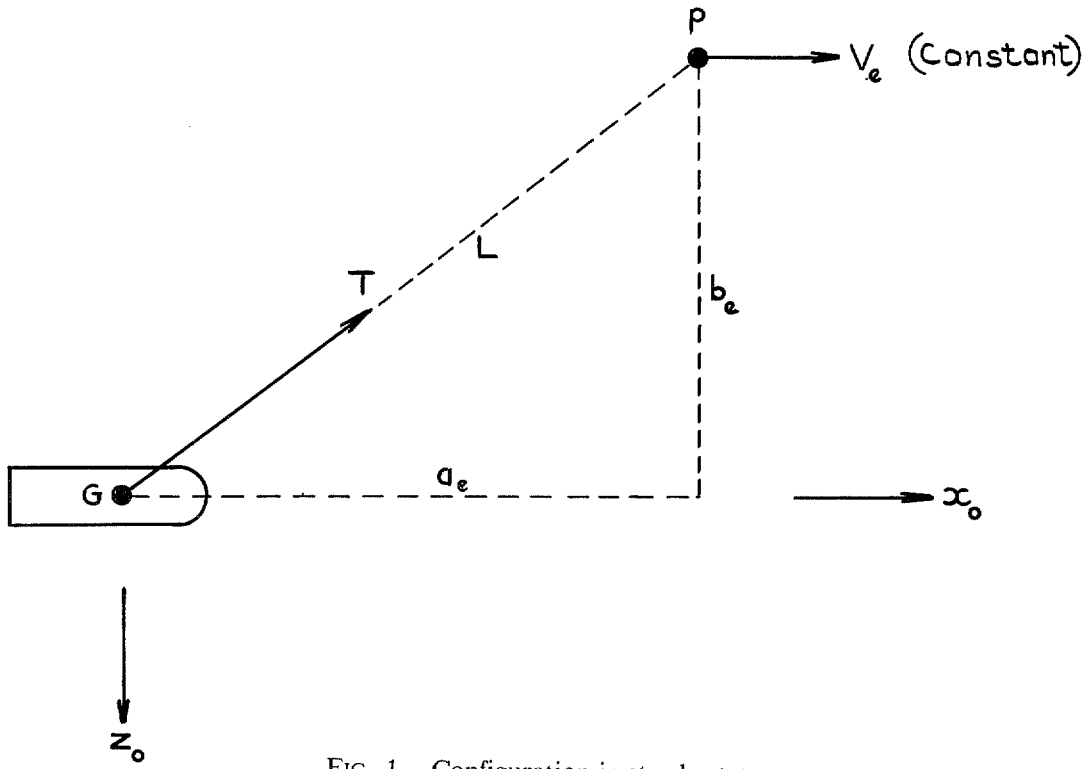

FIG. 1. Configuration in steady state.

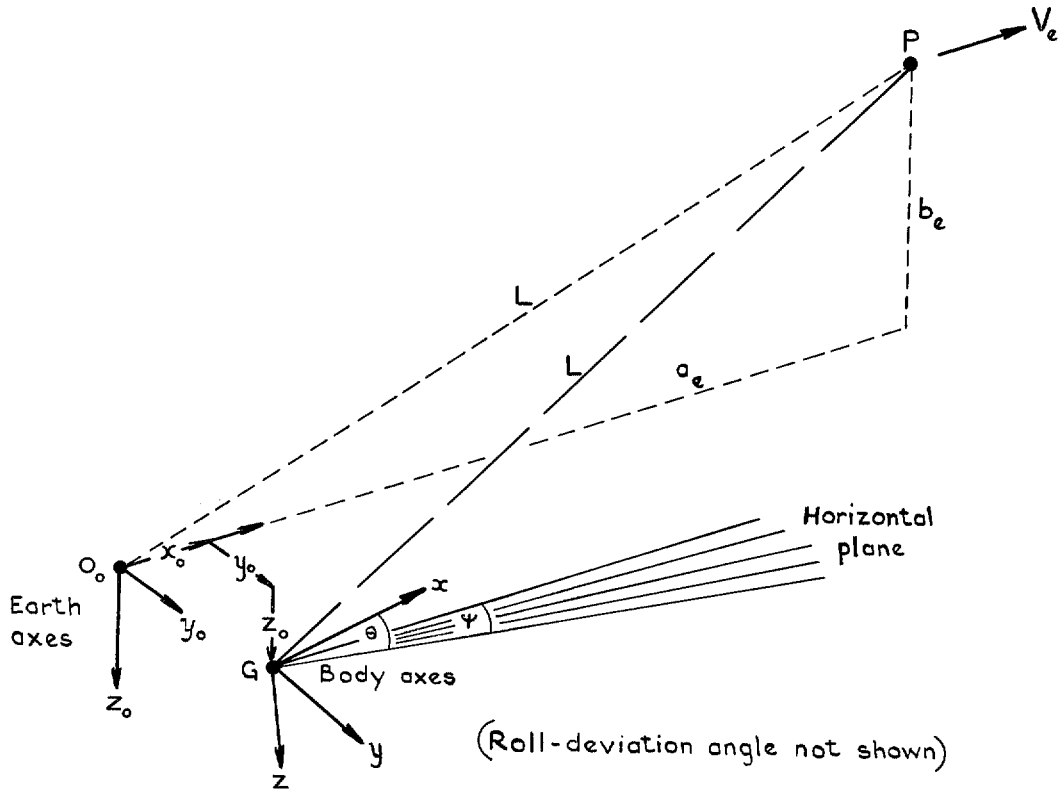

FIG. 2. Geometry of perturbed configuration.

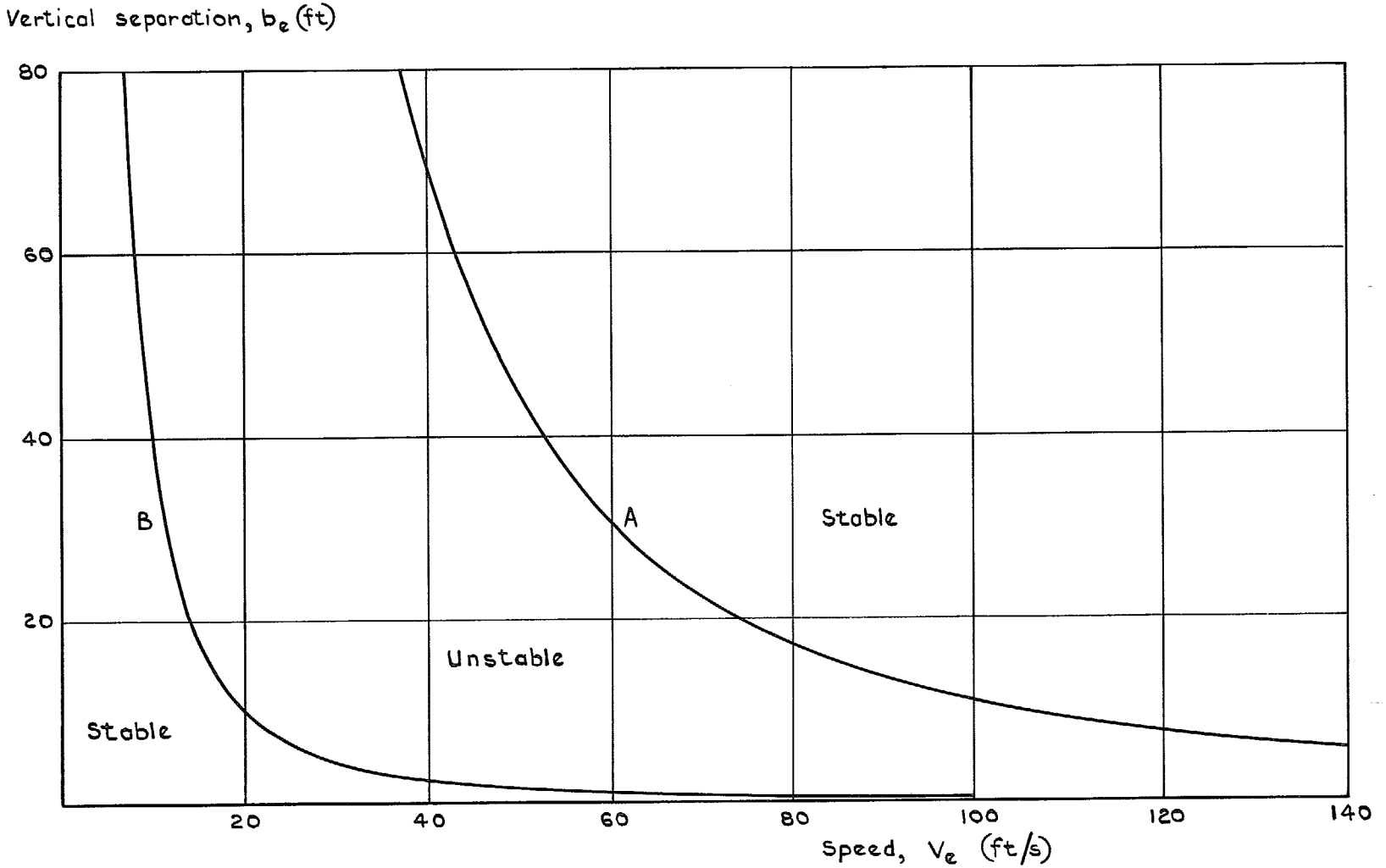

FIG. 3. Typical stability boundaries for given object.

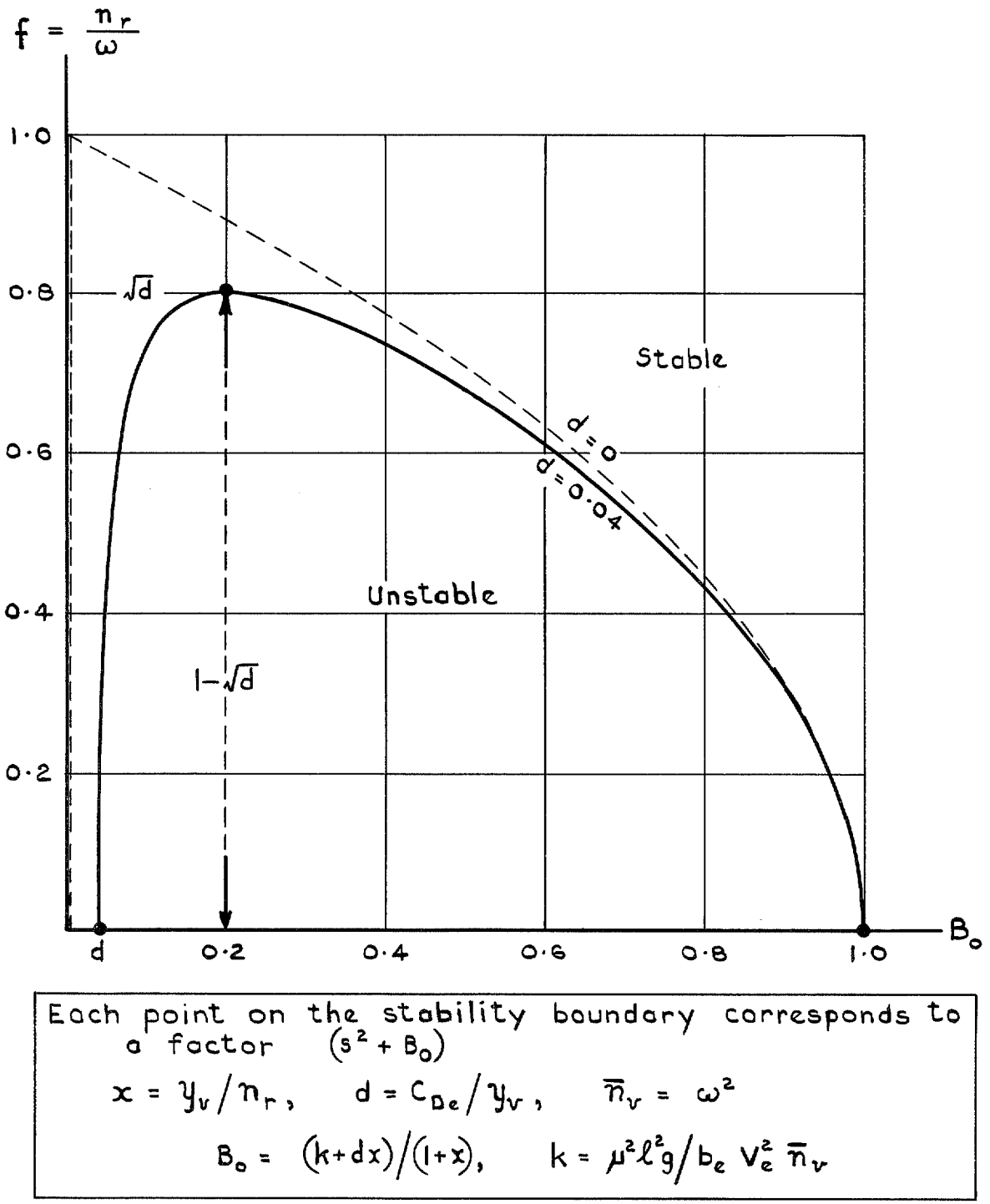

Each point on the stability boundary corresponds to a factor $(s^2 + B_o)$

$$x = y_v / n_r, \quad d = C_{De} / y_v, \quad \bar{n}_v = \omega^2$$

$$B_o = (k + dx)/(1 + x), \quad k = \mu^2 \ell^2 g / b_e V_e^2 \bar{n}_v$$

FIG. 4. Normalised stability boundary (general).

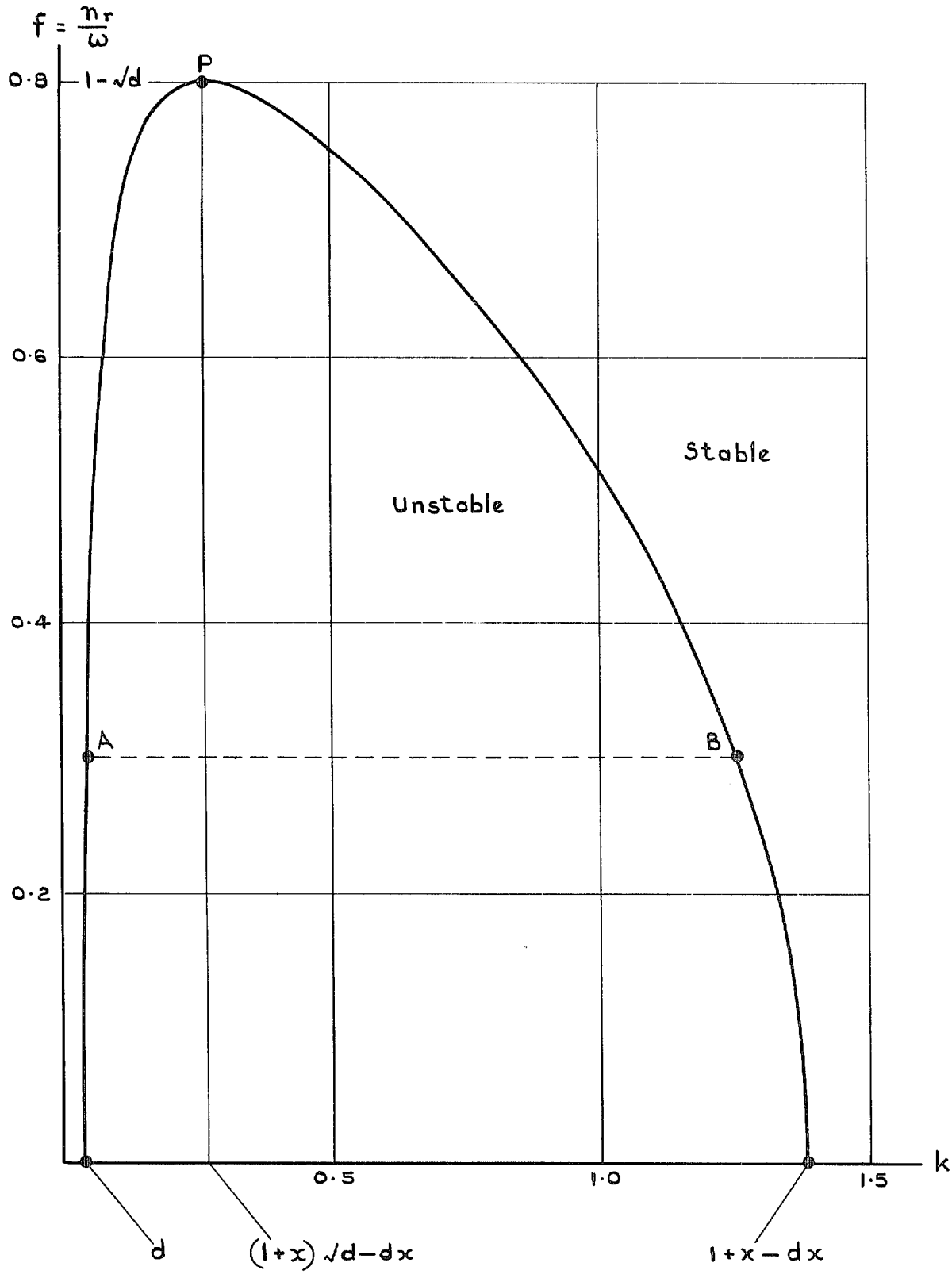

FIG. 5. Stability boundary (general).

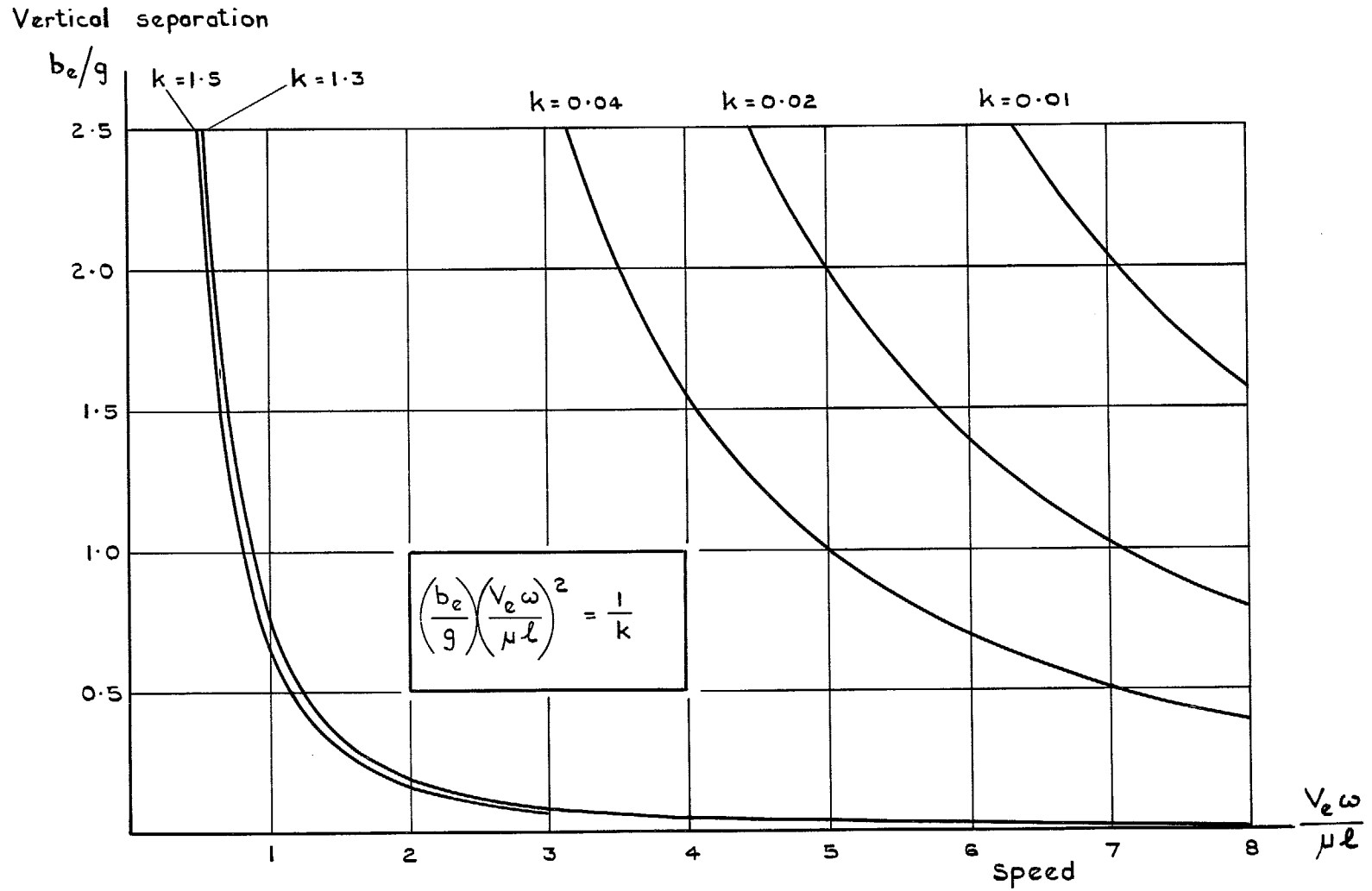

FIG. 6. Family of stability boundaries (varying k).

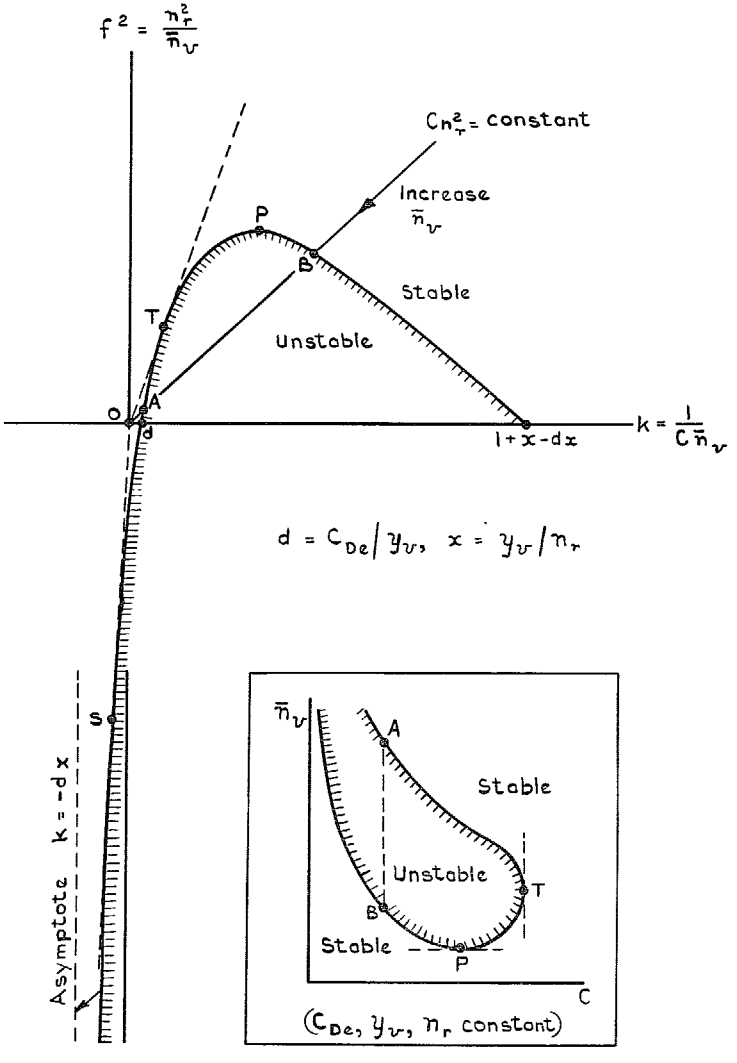

FIG. 7. Stability diagrams for varying $\bar{n}_v$.

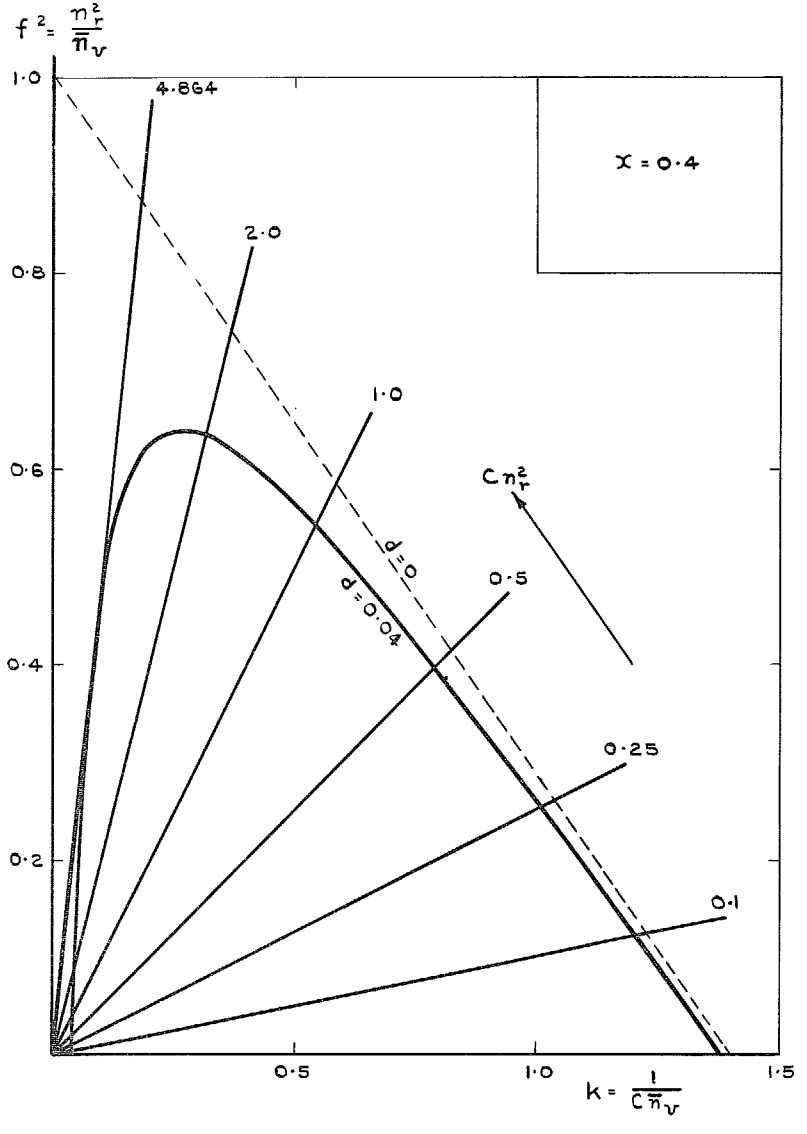

FIG. 8. Stability diagrams for varying $\bar{n}_v$.

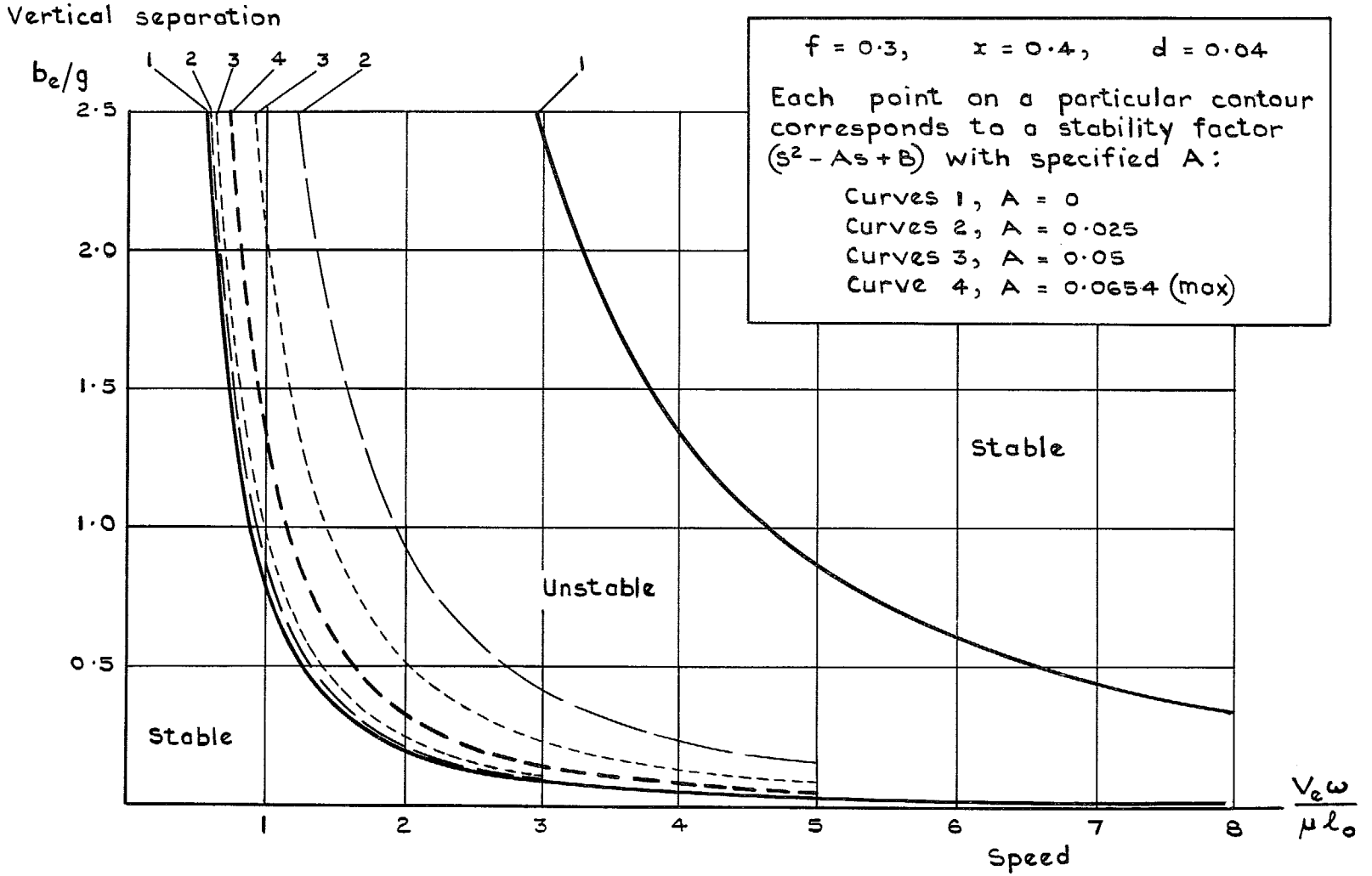

FIG. 9. Stability contour diagram for unstable region.

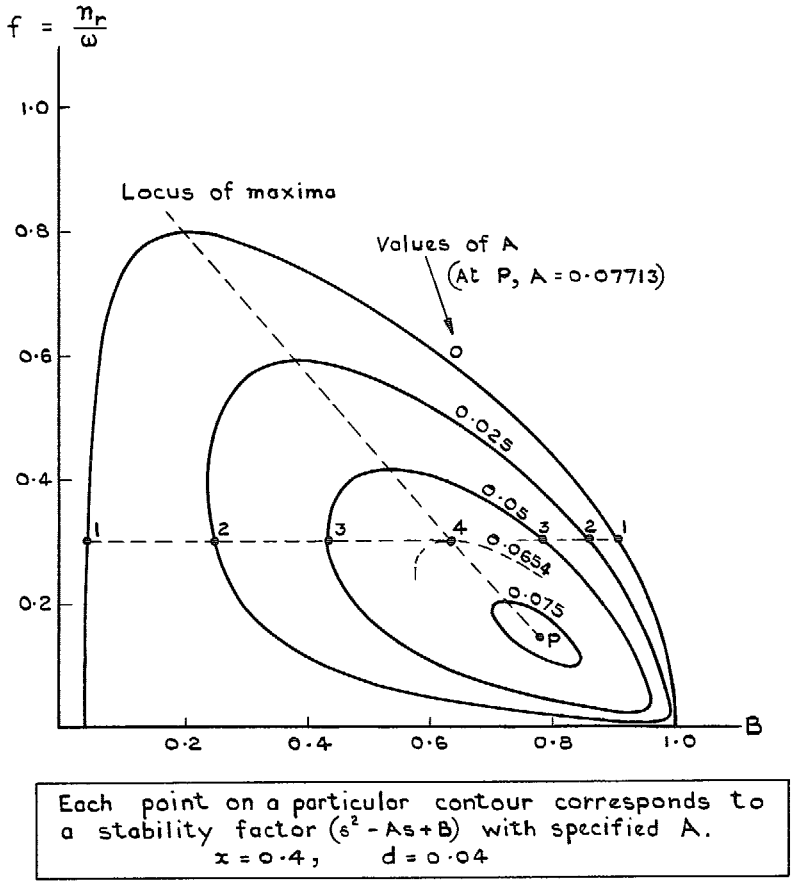

FIG. 10. Normalised stability contour diagram for unstable region.

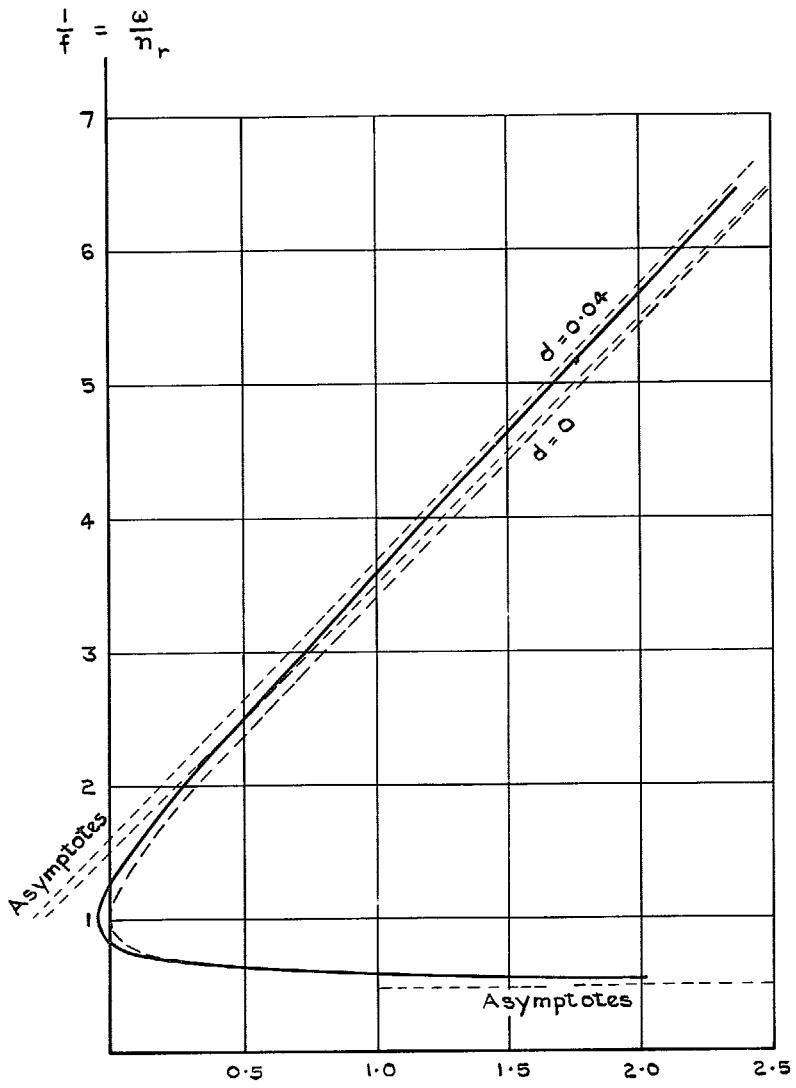

FIG. 11. Graph of function for determining maximum persistence.

Printed in Wales for Her Majesty's Stationery Office by Allens Printers (Wales) Limited.
Dd. 502110 K.5.

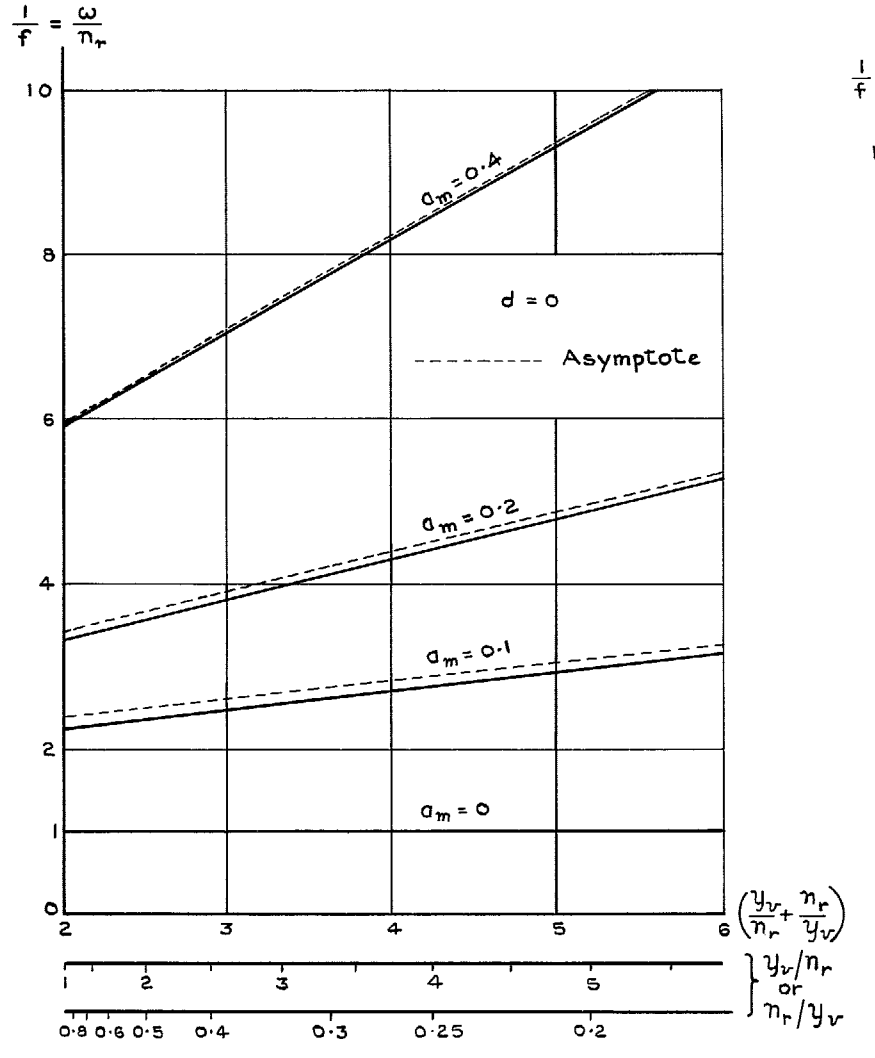

FIG. 12. Loci of maximum persistence.

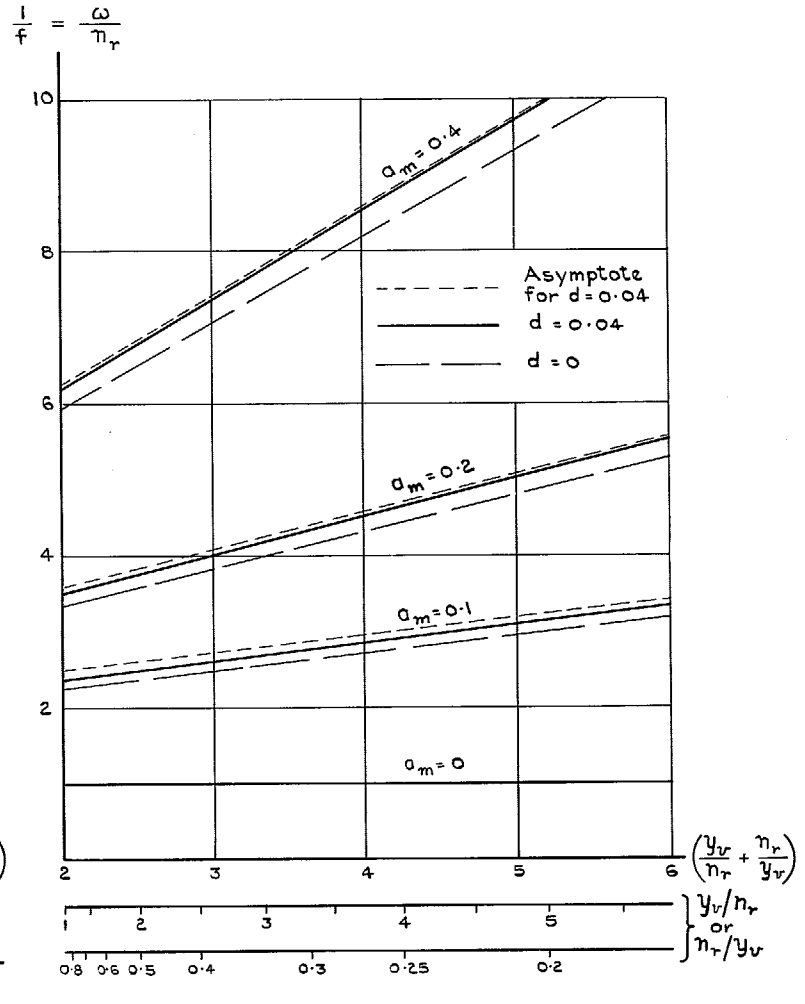

FIG. 13. Loci of maximum persistence.

Published by
HER MAJESTY'S STATIONERY OFFICE

To be purchased from
49 High Holborn, London WC1V 6HB
13a Castle Street, Edinburgh EH2 3AR
109 St. Mary Street, Cardiff CF1 1JW
Brazennose Street, Manchester M60 8AS
50 Fairfax Street, Bristol BS1 3DE
258 Broad Street, Birmingham B1 2HE
7 Linenhall Street, Belfast BT1 4JY
or through booksellers

SBN 11 470415 5